JOURNAL OF SOLID STATE CHEMISTRY 71, 361–370 (1987)

Investigation of Structural States in the Series MGaSiO$_4$, MAlGeO$_4$, MGaGeO$_4$ (M = Na, K)

J. BARBIER AND M. E. FLEET

Department of Geology, University of Western Ontario, London, Ontario, Canada N6A 5B7

Received October 30, 1986; in revised form February 17, 1987

MGaSiO$_4$, MAlGeO$_4$, and MGaGeO$_4$ phases (M = Na, K) have been synthesized using flux, hydrothermal, and melt growth techniques and characterized by TEM and single crystal and powder X-ray diffraction. The K compounds crystallize with a ($2\sqrt{3}A$, C) hexagonal unit cell which is a superstructure of the (A, C) hexagonal kalsilite (KAlSiO$_4$) cell. The room-temperature polymorphs of the Na compounds crystallize with a ($\sqrt{3}A$, $3A$, C, $\gamma \simeq 90°$) monoclinic cell and are isostructural with beryllonite (NaBePO$_4$). TEM data suggest that they transform to a kalsilite-like ($\sqrt{3}A$, C) hexagonal cell at high temperature.

Introduction

The crystal structures of the feldspathoid minerals kalsilite (KAlSiO$_4$) and nepheline (~Na$_3$K(AlSiO$_4$)$_4$) are stuffed-tridymite derivatives (e.g., *1*). They consist of a framework of corner-linked (Al,Si)O$_4$ tetrahedra derived from that of tridymite (SiO$_2$) and containing large interstices filled with K and Na atoms (cf. Fig. 1 and the structure determinations of kalsilite (*2*) and nepheline (e.g., *3–5*)). [It is noteworthy that the tridymite structure itself appears to be stabilized by small amounts of alkali oxides (e.g., *6*, *7*).]

The structural role of the alkali atoms as network modifiers in these alumino-silicate frameworks has been investigated by substituting larger atoms, such as Rb and Cs, and determining the crystal structures of RbAlSiO$_4$ (*8*) and CsAlSiO$_4$ (*1*). In these compounds the topology of the (Al,Si)O$_4$ framework differs from the tridimyte type in order to accommodate the larger alkali cations.

Alternatively, the role of the network-forming Al and Si atoms can be examined by synthesizing Ga- and/or Ge-substituted phases but very little work appears to have been done on such analogs (e.g., *9*). Their detailed study, however, could provide new insights into the complex crystal chemistry of the alumino-silicate phases including, for instance, the question of polymorphism (e.g., *10, 11*). See *Note added in proof.*

Accordingly, a series of compounds including KAlGeO$_4$, KGaSiO$_4$, KGaGeO$_4$, and their Na counterparts have been synthesized (and, for some of them, obtained as single crystals), and the present paper reports on their characterization by X-ray and electron diffraction.

0022-4596/87 $3.00

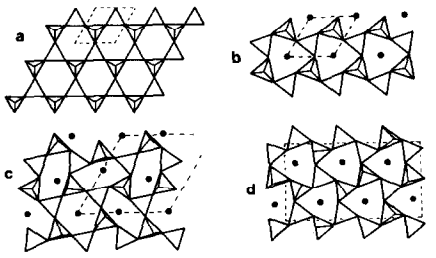

FIG. 1. Schematic representation of the topologies of the tetrahedral frameworks in the structures of tridymite (a), kalsilite (b), nepheline (c), and beryllonite (d). Single (001) layers are drawn and adjacent layers, above and below, are connected via apical oxygen atoms. Note the different topology of the beryllonite structure containing two kinds of six-membered tetrahedral rings.

Experimental

Syntheses were carried out from stoichiometric mixtures of potassium carbonate (Fisher certified grade, 0.008% Na), sodium carbonate (Baker analyzed reagent, 0.0004% K) and high-purity (99.99%) Al_2O_3, Ga_2O_3, SiO_2, and GeO_2 powders.

Single crystal growth experiments used either a flux technique following the procedure described by Ozima and Akimoto (*12*) or a hydrothermal process. In the first case, the carbonate plus oxide starting materials were mixed with a molybdeno-vanadate flux (composition in mole%: 51.7% K_2O (or Na_2O), 42.3% MoO_3, and 6.5% V_2O_5) in a ratio of 1 : 13 by weight. The mixtures were contained in Pt crucibles with tight-fitting lids, soaked at 1000°C for 5 days, cooled to 600°C at 1°C/hr, and quenched in air. The crystallized products were separated from the flux by dissolution of the latter in hot water.

In the case of the hydrothermal growth experiments, the decarbonated oxide mixtures were sealed in gold capsules together with a small amount of 3*M* KOH (or NaOH) aqueous solution and held at constant pressure (about 1 kbar, in a cold-sealed bomb) and temperature (in the range 500–800°C) for a duration of 1 to 2 weeks.

Direct high-temperature syntheses were also carried out for some compositions including $KGaGeO_4$, $NaGaGeO_4$, and $NaAlGeO_4$. For this purpose, the carbonate plus oxide mixtures were pressed into pellets, decarbonated at 700°C, repelletized, melted at 1200°C for one hour, furnace-cooled to 1000°C, and quenched in air.

The nature of the reaction products was checked by powder X-ray diffraction (with a Rigaku Geigerflex diffractometer), single crystal precession technique and electron diffraction (with a Hitachi 800 electron microscope operating at 200 kV and equipped with a ±60° rotation–tilt goniometer stage). All products appeared to be very sensitive to electron beam damage so that examination of samples by electron microscopy was only possible at low magnification (up to about 80,000×) thereby precluding direct imaging of lattice fringes.

Results

Flux growth and hydrothermal syntheses yielded microcrystalline products (grain size $\leqq 50$ μm) for all compositions as well as sizeable single crystals for $KGaGeO_4$, $KGaSiO_4$, $NaGaGeO_4$, and $NaAlGeO_4$. However, the crystals of the Na phases were invariably twinned (showing a sector-twinned pseudo-hexagonal morphology; cf. Fig. 2) and only in the case of $NaGaGeO_4$ were the crystals large enough to allow separation of the twin individuals and determination of the structure (*13*).

On the basis of the unit-cell data determined in the present study, the K and Na compounds form two distinct groups of isostructural phases and only the latter show indications of polymorphism over the temperature range investigated here (500–1000°C). For convenience, the products of the crystal growth experiments and the

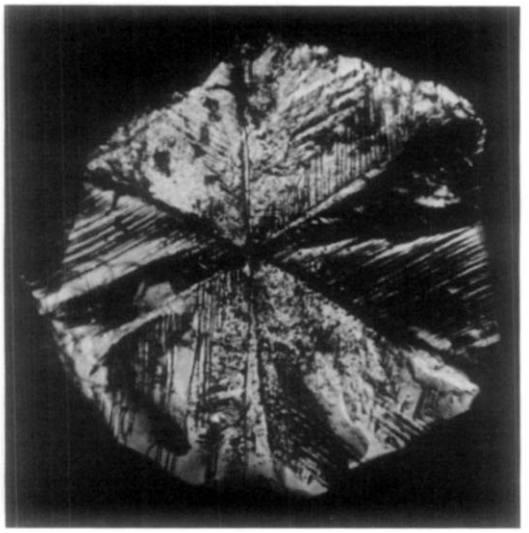

FIG. 2. Optical micrograph (crossed polars) of a hydrothermally grown $NaAlGeO_4$ crystal quenched from 800°C. The sector-twinned pseudo-hexagonal morphology results from the growth of three beryllonite-type crystals rotated by 120°. The lamellar twinning within individual sectors corresponds to the orthorhombic → monoclinic transition taking place during quenching.

high-temperature syntheses will be referred to as "low-temperature" and "high-temperature" phases, respectively.

1. Unit-Cell Data for the K Compounds

Electron diffraction data from $KGaGeO_4$ synthesized at high temperature (Fig. 3) show that it crystallizes with a hexagonal unit cell which is a supercell of the kalsilite cell. Its cell dimensions are expressed as

$$a = 2\sqrt{3}A, \quad c = C,$$

where A (≃5.3 Å) and C(≃8.6 Å) refer to the kalsilite subcell. The relative orientation of the cell and subcell is schematically shown in Fig. 4. The same hexagonal cell was also determined from X-ray precession data for a flux-grown $KGaGeO_4$ single crystal, the extinction conditions [000l, $l \neq 2n$] being consistent with the space groups $P6_3$ or $P6_322$. [Note that, in Fig. 3a, the 0001 and 0003 reflections arise from multiple electron diffraction.]

Powder diffraction data from the low-temperature phases $KGaGeO_4$, $KAlGeO_4$, and $KGaSiO_4$ also yielded similar unit cells and the corresponding cell parameters are listed in Table I. It should be pointed out that the present powder patterns are very similar to that of $KAlGeO_4$ published by Kivlighn (*9*) who, however, indexed it on a smaller orthorhombic cell with the parameters $a = 9.260$, $b = 16.017$, and $c = 8.636$ Å.

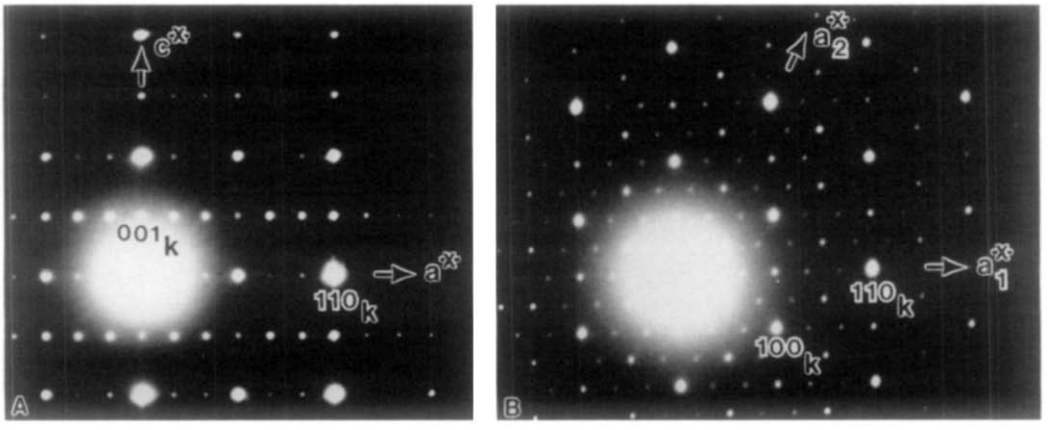

FIG. 3. [11$\bar{2}$0] (a) and [0001] (b) zone-axis electron diffraction patterns from $KGaGeO_4$ microcrystals quenched from 1000°C, corresponding to an hexagonal ($2\sqrt{3}A$, C) unit cell. Note the strong kalsilite (A, C) subcell (subscript "k") and the medium-strong ($2A$, C) subcell.

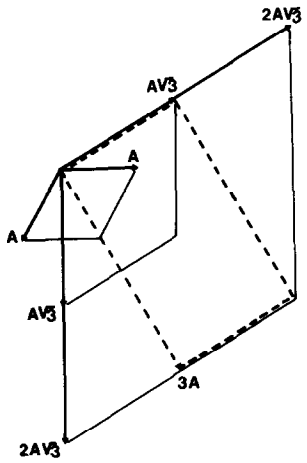

FIG. 4. Geometric relationships between the (A, C) kalsilite cell and the hexagonal and beryllonite-type unit cells identified for the K and Na compounds.

TABLE I

UNIT-CELL PARAMETERS FOR THE K COMPOUNDS REFINED FROM X-RAY POWDER DIFFRACTION DATA ($\lambda_{CuK\alpha_1}$ = 1.5406 Å)

	a (Å)	c (Å)
$KGaSiO_4$	18.172(3)	8.528(2)
$KAlGeO_4$	18.385(2)	8.579(2)
$KGaGeO_4$	18.543(2)	8.668(2)

2. *Unit-Cell Data for the Na Compounds*

A structure refinement carried out on a flux-grown $NaGaGeO_4$ single crystal (*13*) established that it is isostructural with beryllonite $NaBePO_4$ (*14*) and $CaAl_2O_4$ (*15*). Powder X-ray diffraction patterns of low-temperature $NaGaGeO_4$, $NaAlGeO_4$, and $NaGaSiO_4$ could also all be indexed on a monoclinic beryllonite-type unit cell with the parameters listed in Table II. All cells show a marked orthohexagonal character with $\gamma \simeq 90°$ and $b/a \simeq \sqrt{3}$ which explains the tendency for these phases to grow as sector-twinned pseudo-hexagonal crystals. [A similar observation has been reported in the case of $RbAlSiO_4$ crystals (*8*).]

Kivlighn (*9*) synthesized $NaAlGeO_4$ by recrystallization from a glass at 800°C and obtained the following orthorhombic unit cell: a = 8.872, b = 14.874, c = 8.278 Å. Although somewhat different from our data in Table II, it is still consistent with a beryllonite-type structure.

The parameters of the beryllonite-type cells can be expressed in terms of the (A, C) kalsilite parameters as follows (cf. Fig. 4): $a = \sqrt{3}A$, $b = 3A$, $c = C$, $\gamma \simeq 90°$, with $A \simeq$ 5.1 Å and $C \simeq$ 8.3 Å.

It should be noted, however, that the framework topology in the beryllonite structure differs from that in the kalsilite (or nepheline) structure (cf. Fig. 1), the highest

TABLE II

UNIT-CELL PARAMETERS FOR THE BERYLLONITE-TYPE Na COMPOUNDS REFINED FROM X-RAY POWDER DIFFRACTION DATA ($\lambda_{CuK\alpha_1}$ = 1.5406 Å)

	a (Å)	b (Å)	c (Å)	γ (°)	b/a	Reference
$NaGaGeO_4$(low T)	8.816(3)	15.616(4)	8.234(3)	90.18(3)	1.771	This work
$NaGaGeO_4$(high T)	8.919(5)	15.664(8)	8.336(6)	90	1.756	This work
$NaAlGeO_4$(low T)	8.803(4)	15.360(3)	8.235(3)	90.15(3)	1.745	This work
$NaAlGeO_4$(high T)	8.813(2)	15.300(3)	8.342(2)	90	1.736	This work
$NaGaSiO_4$(low T)	8.734(4)	15.302(6)	8.256(5)	90.23(5)	1.752	This work
$NaBePO_4$ (single crystal)	8.178	14.114	7.819	90.0	1.725	(*14*)
$CaAl_2O_4$ (single crystal)	8.700	15.191	8.092	90.28	1.746	(*15*)

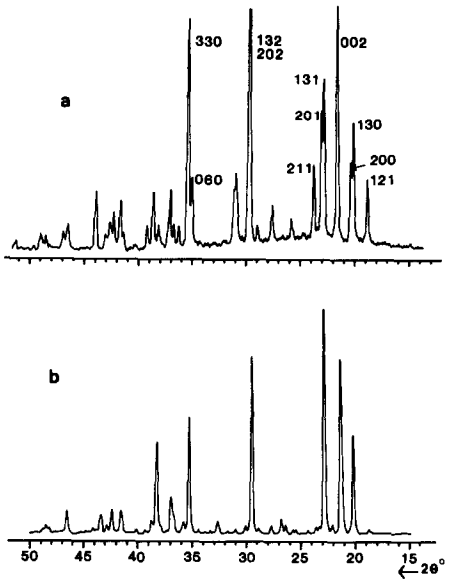

FIG. 5. X-ray powder diffraction patterns for the low-temperature (a) and high-temperature (b) $NaAlGeO_4$ phases. Note the orthorhombic line splitting in (a) and the strong hexagonal subcell in (b).

symmetry of the former being orthorhombic (*16*). It follows that the structure of the low-temperature Na compounds is not a simple superstructure of the kalsilite type which is consistent with the absence of kalsilite subcell reflections in the single crystal X-ray diffraction patterns.

Refinement of powder X-ray diffraction data from the high-temperature $NaGaGeO_4$ and $NaAlGeO_4$ phases also led to beryllonite-type cells (Table II) with, however, a lesser degree of orthorhombic distortion reflected in smaller b/a ratios approaching the ideal value of $\sqrt{3}$ for an orthohexagonal cell. This change in cell dimensions was most clearly observed in the case of $NaAlGeO_4$ as shown in Fig. 5: the splitting of pairs of diffraction lines, such as (200)/(130) and (060)/(330), has become negligible in the pattern of the high-temperature phase which also shows a strong hexagonal subcell with the parameters $a = 8.81$ Å and $c = 8.35$ Å, i.e., $a = \sqrt{3}A$ and $c = C$.

The strong pseudo-hexagonal character of the $NaAlGeO_4$ unit cell at high temperature was also revealed by the TEM observation of triply-twinned microcrystals. A typical [001] electron diffraction pattern of such crystals is shown in Fig. 6: although dimensionally hexagonal, it lacks six-fold symmetry in the intensity distribution of the weak reflections indicating that it results, in fact, from the superposition of three equivalent orthorhombic patterns ($\sqrt{3}A$, $3A$, C beryllonite cell) rotated by 60°. [Note that the strong ($\sqrt{3}A$, C) hexagonal subcell in Fig. 6 is the same as that observed in the X-ray powder pattern in Fig. 5b.] The pseudo-hexagonal symmetry is generated by twinning of the beryllonite structure on the (130) and (110) planes and is equivalent to that observed, on a macroscopic scale, in the sector-twinned single crystals of the Na compounds (cf. Fig. 2).

A similar twinning was also present in $NaGaGeO_4$ crystals quenched from high temperature: the electron diffraction pattern in Fig. 7 shows two sets of sharp reflections originating from a beryllonite crystal twinned on (110) (so that the $[110]_1^*$ and $[110]_2^*$ directions coincide; cf. Fig. 6). The streaking parallel to [110]* is associated with the fine scale intergrowth of the two twin individuals, the composition plane

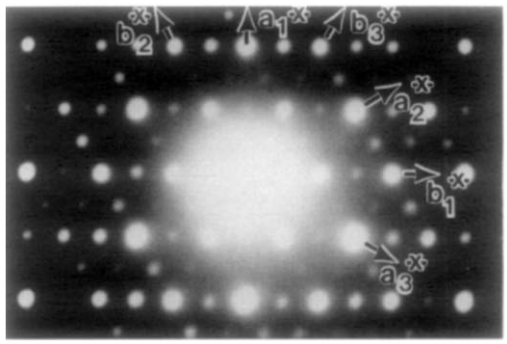

FIG. 6. [001] electron diffraction pattern of a triply twinned beryllonite-type $NaAlGeO_4$ crystal quenched from 1000°C. Note the strong kalsilite-type (A, C) and the medium-strong ($\sqrt{3}A$, C) hexagonal subcells.

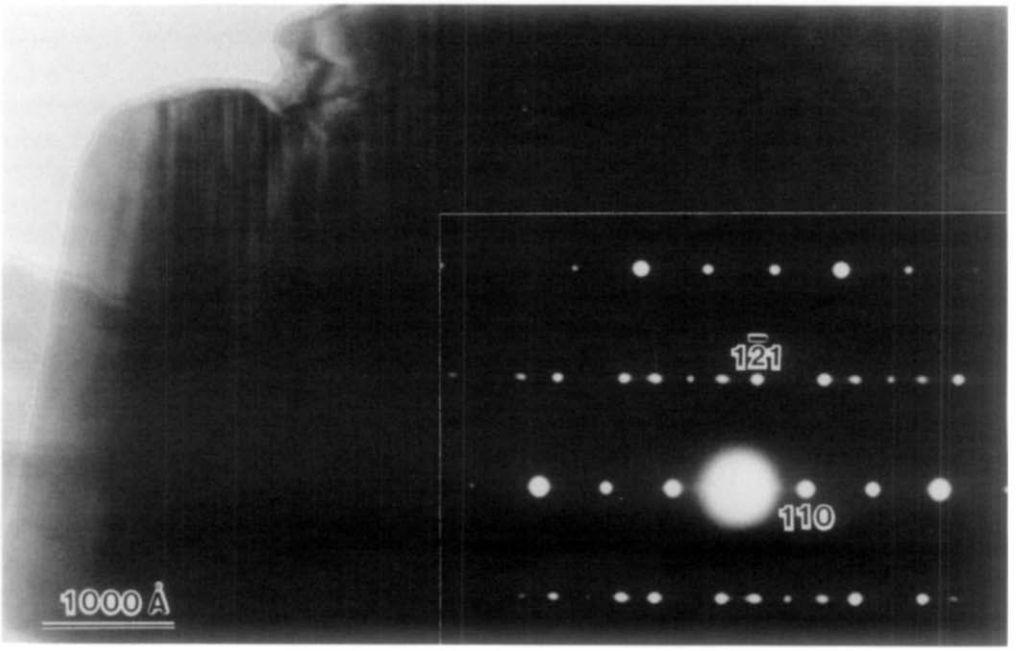

FIG. 7. [$\bar{1}$13]-zone image of the fine-scale intergrowth of two beryllonite-type $NaGaGeO_4$ crystals twinned on (110) [sample quenched from 1000°C].

being parallel to (110) (coherent reflection twinning).

The (pseudo-)orthorhombic unit cells of the high-temperature $NaAlGeO_4$ and $NaGaGeO_4$ phases (cf. Table II) suggest that a monoclinic → orthorhombic transition may take place at high temperature in the beryllonite structure. Such a transformation would be consistent with the frequent (100) faulting observed in $NaGaGeO_4$ (Fig. 8) corresponding to the formation of thin twin lamellae during quenching. The same lamellar twinning was also observed optically, on a coarser scale, in $NaGaGeO_4$ and $NaAlGeO_4$ single crystals (cf. Fig. 2) indicating that the orthorhombic → monoclinic transformation occurs below the quenching temperature (e.g., 600°C for flux-grown $NaGaGeO_4$ crystals).

Along with the beryllonite-type crystals, the high-temperature $NaGaGeO_4$ phase also contained crystals with a smaller ($\sqrt{3}A$, C) hexagonal unit cell (i.e., the hexagonal cell equivalent to the beryllonite cell; cf. Fig. 4) which were commonly faulted on at least one set of {100} planes (Fig. 9). As discussed in the next section, this result together with the presence of beryllonite crystals faulted on (010) (Fig. 10) suggests the existence of a high-temperature kalsilite-like hexagonal polymorph for the Na compounds.

Discussion

All unit cells determined in the present study for the series of compounds $M GaSiO_4$, $M AlGeO_4$, and $M GaGeO_4$ (M = K, Na) are consistent with tetrahedral framework structures with topologies related to those of the unsubstituted $M AlSiO_4$ phases.

Single crystal data show that the room-temperature polymorphs of the substituted Na compounds crystallize with the beryllonite ($NaBePO_4$) structure (cf. structure

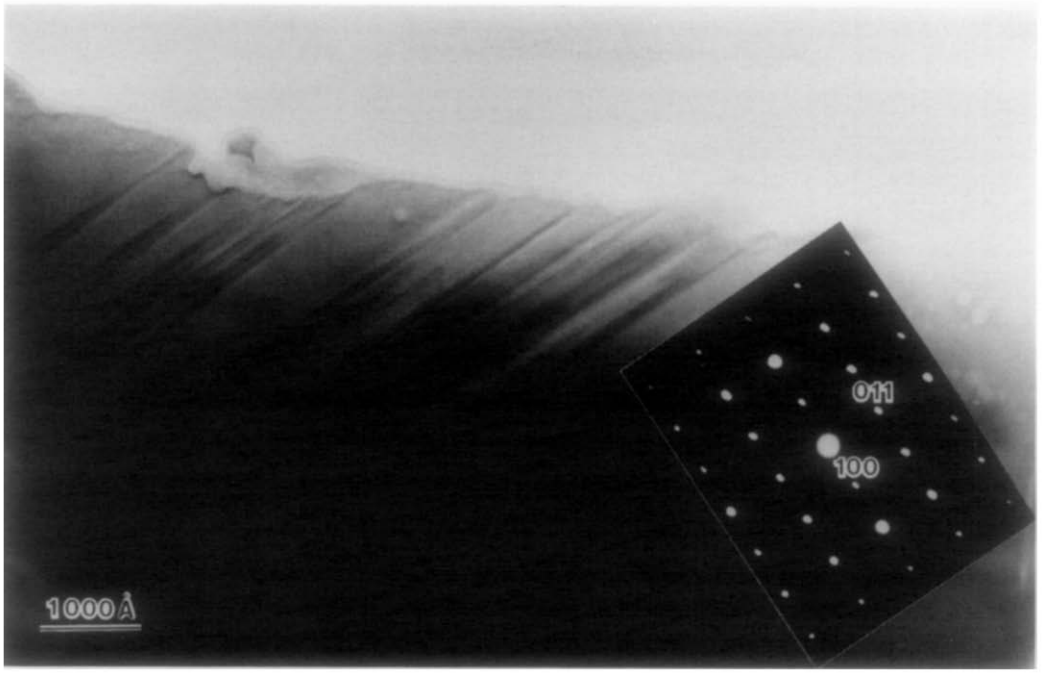

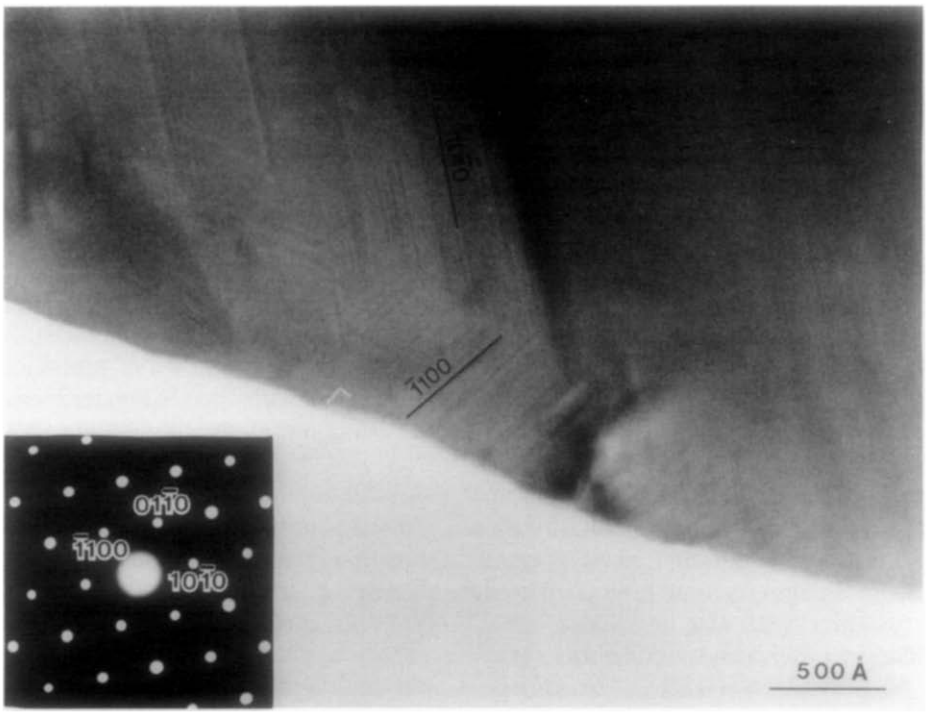

FIG. 9. [0001]-zone image of a ($\sqrt{3}A$, C) hexgonal crystal in the high-temperature $NaGaGeO_4$ phase. Faults are visible parallel to the three equivalent $(10\bar{1}0)$ planes, possibly corresponding to the growth of the beryllonite-type structure.

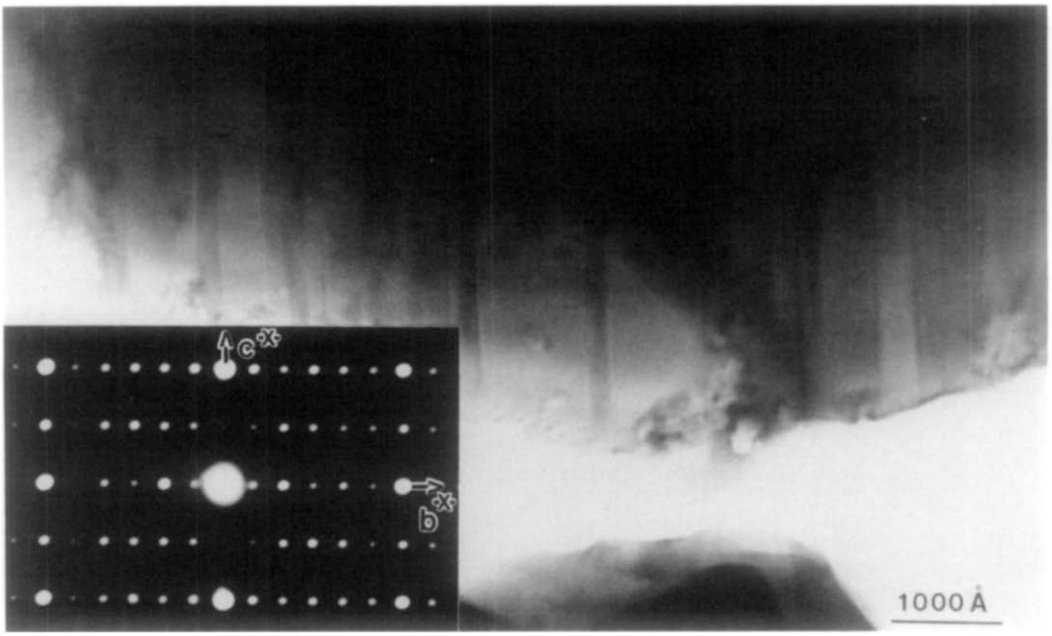

FIG. 10. [100]-zone image of a beryllonite-type $NaAlGeO_4$ crystal quenched from 1000°C containing domains separated by (010) faults. Note the change of contrast at the boundaries revealing the twin nature of adjacent domains.

determination of $NaGaGeO_4$ by Fleet and Barbier (*13*)). It is noteworthy, however, that this particular structure type has not been reported with certainty in the case of $NaAlSiO_4$. [We note that Liebau (*1*) quotes some data referring to a beryllonite-type synthetic $NaAlSiO_4$ phase but apparently no structure determination has been published.] Nevertheless, it is generally recognized that the topology of a particular framework compound depends primarily on the relative sizes of the cavity and framework atomic species (e.g., *1*). On that basis, it is not clear why $NaAlSiO_4$ (with a mean T–O bond length of 1.70 Å, as calculated from Shannon's ionic radii (*17*)) could not crystallize with the beryllonite structure like the other compounds of the series, i.e., $NaBePO_4$, $NaGaSiO_4$, $NaAlGeO_4$, and $NaGaGeO_4$ (with mean T–O bond lengths of 1.60, 1.74, 1.77, and 1.81 Å, respectively). As has been suggested before (*5*), it appears indeed possible that the beryllonite structure is the stable form for pure, stoichiometric $NaAlSiO_4$ while the commonly observed nepheline structure is only stabilized by either small amounts of potassium (in $Na_{1-x}K_xAlSiO_4$) or vacancies (in nonstoichoimetric $Na_{1-x}Al_{1-x}Si_{1+x}O_4$).

Results from the present study indicate that the following series of transitions may take place with increasing temperature in the Na compounds: monoclinic ($\sqrt{3}A$, $3A$, C, $\gamma \simeq 90°$) → orthorhombic ($\sqrt{3}A$, $3A$, C) → hexagonal ($\sqrt{3}A$, C). The first transformation simply corresponds to a slight distortion of the beryllonite structure and is displacive in nature. The second one, however, must be reconstructive and involves a change in the topology of the tetrahedral framework since the highest symmetry of the beryllonite topology is orthorhombic (*16*). Based on our TEM data and on the simple relationship between the

two structure types (cf. below), it is proposed that the topology change is from the beryllonite to the kalsilite type.

As depicted in Fig. 11 (for the idealized topology), the beryllonite structure can be described as a stacking along the *b* direction of identical slabs with the kalsilite structure (cf. Fig. 1). Adjacent slabs are twin-related via a two-fold rotation axis parallel to the *c* axis and the composition plane is $(010)_{ber} = (110)_{kal} = (100)_{hex}$ (where the ber, kal, and hex subscripts refer to the beryllonite, kalsilite, and $(\sqrt{3}A, C)$ hexagonal cells, respectively; cf. Fig. 11). An even simpler description recognizes that the composition planes are also antiphase boundaries of the type $(100)_{kal}$, $c/2$ so that the beryllonite structure merely results from the insertion of periodic antiphase boundaries in the kalsilite structure. [Obviously, the complete transformation involves additional tilting of the tetrahedra and shifting of the alkali atoms.]

From the above structural relationship, it is clear that a transformation from a kalsilite-like structure (i.e., with the same topology as kalsilite but possibly very distorted; cf. nepheline) with a $(\sqrt{3}A, C)$ hexagonal unit cell into a beryllonite-type structure would involve faulting on $(100)_{hex}$ and $(010)_{ber}$ planes. This type of faulting has indeed been observed experimentally in $NaGaGeO_4$ and $NaAlGeO_4$ phases quenched from high temperature (cf. Figs. 8 and 9). As well, such a transformation could account for the common occurrence of beryllonite crystals twinned on (130) and (110) (cf. Figs. 6 and 7): this twin law would naturally result from the "growth" of the beryllonite structure along two or three equivalent [210] directions of the $(\sqrt{3}A, C)$ hexagonal structure.

The fact that the beryllonite-type Na compounds are isostructural with $CaAl_2O_4$ is consistent with the predominant role of the relative sizes of the cavity and framework atoms in determining the topology of this class of compounds. Based on Shannon's ionic radii (*17*), the ^{VII}Na–O bond (2.50 Å) and the mean ^{IV}T–O bonds (1.75–1.81 Å) for the Na phases are very similar to, respectively, the ^{VII}Ca–O (2.44 Å) and ^{IV}Al–O (1.77 Å) bonds for $CaAl_2O_4$. [The seven-fold coordination for the Na (Ca) atoms represents an average coordination number in the beryllonite structure (cf. *13, 14, 15*).] It is therefore not unexpected that the accommodation of Na and Ca atoms in TO_4 and AlO_4 frameworks, respectively, requires the same tetrahedral topology.

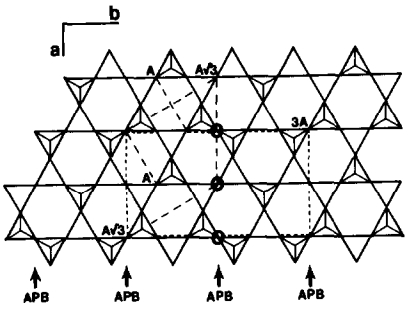

FIG. 11. [001] projection of the (idealized) beryllonite framework showing the relationship with the kalsilite structure. Individual slabs between two adjacent antiphase boundaries (APB) have the kalsilite topology and are related by a shift of $\pm c/2$ or by a two-fold rotation axis parallel to the *c* axis. Several two-fold axes are indicated by circles in the figure. The geometrical relationship between the beryllonite cell, the kalsilite-like $(\sqrt{3}A, C)$ hexagonal cell and the kalsilite (A, C) cell is shown.

Structure determinations of $SrAl_2O_4$ (*18*) and $BaAl_2O_4$ (*19*) have shown that the substitution of Ca by larger atoms causes a change in framework topology and leads to kalsilite-type structures with nine-coordinated Sr and Ba atoms. Based on the isotypy of $NaGaGeO_4$ and $CaAl_2O_4$ and on the similarity of the ^{IX}K–O (2.93 Å) and ^{IX}Ba–O (2.85 Å) bonds, one can reasonably assume that $KGaGeO_4$ and $BaAl_2O_4$ should be structurally very similar. This is supported by our unit-cell data for the K compounds (cf. Table I) indicating a kalsilite-like $(2\sqrt{3}A, C)$ hexagonal cell with a strong

($2A$, C) hexagonal subcell (cf. Fig. 3) which is similar to the hexagonal cell (a = 10.470 Å = $2A$, c = 8.819 Å = C) determined for $BaAl_2O_4$ (*19*). The ($\sqrt{3}$) superstructure in the basal plane in the K compounds could result from Ga/Ge ordering on the tetrahedral sites as has been found in beryllonite-type $NaGaGeO_4$ (*13*). Work is now in progress in order to determine the crystal structure of the K phases using a flux-grown $KGaGeO_4$ single crystal.

Note added in proof. After acceptance of this article for publication, we have become aware of previous single crystal X-ray studies on the same Na and K compounds (*20, 21*) with results consistent with ours.

References

1. F. Liebau, "Structural Chemistry of Silicates," Springer-Verlag, Berlin/Heidelberg/New York/Tokyo (1985).
2. A. J. Perrotta and J. V. Smith, *Mineral. Mag.* **35,** 588–595 (1965).
3. T. Hahn and M. J. Buerger, *Z. Kristallogr.* **106,** 308–338 (1955).
4. W. A. Dollase, *Z. Kristallogr.* **132,** 27–44 (1970).
5. M. Gregorkiewitz, *Bull. Mineral.* **107,** 499–507 (1984).
6. O. W. Flörke, *Naturwiss.* **43,** 419 (1956).
7. S. B. Holmquist, *J. Amer. Ceram. Soc.* **44,** 82–86 (1961).
8. R. Klaska and O. Jarchow, *Z. Kristallogr.* **142,** 225–238 (1975).
9. H. D. Kivlighn, Jr., *J. Amer. Chem. Soc.* **49**(3), 148–151 (1966).
10. L. P. Cook, R. S. Roth, H. S. Parker, and T. Negas, *Amer. Miner.* **62,** 1180–1190 (1977).
11. R. N. Abbott, Jr., *Amer. Miner.* **69,** 449–457 (1984).
12. M. Ozima and S. Akimoto, *Amer. Miner.* **68,** 1199–1205 (1983).
13. M. E. Fleet and J. Barbier, *Z. Kristallogr.* (in press).
14. G. Giuseppetti and C. Tadini, *Tschermaks Min. Petr. Mitt.* **20,** 2–12 (1973).
15. W. Hörkner and H. K. Müller-Buschbaum, *J. Inorg. Nucl. Chem.* **38,** 983–984 (1976).
16. J. V. Smith, *Amer. Miner.* **62,** 703–709 (1977).
17. R. D. Shannon, *Acta Crystallogr. A* **32,** 751–767 (1976).
18. A. R. Schulze and H. K. Müller-Buschbaum, *Z. Anorg. Allg. Chem.* **475,** 205–210 (1981).
19. W. Hörkner and H. K. Müller-Buschbaum, *Z. Anorg. Allg. Chem.* **451,** 40–44 (1979).
20. R. Klaska, K. H. Klaska, and O. Jarchow, *Z. Kristallogr.* **149,** 135–137 (1979).
21. P. A. Sandomirskii, S. S. Meshalkin, I. V. Rozhdestvenskaya, L. N. Dem'yanets, and T. G. Uvarova, *Sov. Phys. Crystallogr.* **31**(5), 522–527 (1986).